Journal of Nuclear Materials 384 (2009) 25–29

Contents lists available at ScienceDirect

Journal of Nuclear Materials

journal homepage: www.elsevier.com/locate/jnucmat

Oxygen effects on irradiated tantalum alloys

P. Hosemann [a,b,*], S.A. Maloy [a], R.R. Greco [a], J.G. Swadener [a], T. Romero [a]

[a] Los Alamos National Laboratory, P.O. Box 1663, Los Alamos, 87544 NM, USA
[b] University of Leoben, Franz-Josef-Strasse 18, 8700 Leoben, Austria

ARTICLE INFO

Article history:
Received 4 February 2008
Accepted 28 September 2008

ABSTRACT

Ta and Ta–1% W are being considered to be used as target clad materials in the LANSCE proton beam line for the material test station (MTS). To investigate the embrittlement of these materials due to oxygen contamination and proton irradiation, Ta and Ta–1 wt% W (as received and with ~400 ppm O) were exposed to a 3.5 MeV proton beam at the ion beam materials laboratory at LANL. After irradiating the samples in the proton beam, nanoindentation was performed in cross-section to investigate the hardness increase of the materials due to irradiation. The nanoindentation showed that the hardness increase due to irradiation is between 9% and 20% depending on the material. The results show good agreement with mechanical testing results on tantalum and Ta–1 wt% W after high energy proton irradiation to doses up to 23 dpa.

Published by Elsevier B.V.

1. Introduction

Tantalum is a refractory metal with many desirable properties for use as a spallation target. It has a high melting temperature and high density coupled with ductility at room temperature. It is also corrosion resistant in water and under irradiation from experience using it as a spallation target at 50–100 °C. In addition, pure tantalum (>99.99% wt%) has shown retention of ductility after irradiation at ISIS to a dose of 11 dpa at irradiation temperatures below 200 °C and tested after irradiation at 25 and 250 °C. Strain to necking still measured above 11% (Chen et al., 2001, 2003) [1,2]. On the other hand, previous results [3,4] of testing tantalum with higher impurity content after irradiation in a high energy proton beam show a reduction of uniform elongation to less than 1% after irradiation to less than 0.5 dpa. In addition, a much higher hardening rate was observed when compared to the data of Chen et al. [1].

Thus, Ta (in the following designated as pure tantalum) and Ta1W (tantalum with 1 wt% W) are being considered as target clad materials for the material test station (MTS) at the Los Alamos Neutron Science Center (LANSCE) proton beam line at the Los Alamos National Laboratory (LANL). At elevated temperatures, during processing or welding, tantalum can pick up a significant amount of oxygen based on its oxygen solubility [5]. To study the effects of oxygen on irradiation hardening in these alloys, the hardening of pure tantalum and Ta–1 wt% W due to irradiation has been studied for alloys in the as-received condition and after addition of ~400 ppm oxygen through performing nanoindentation testing in cross-section after ion irradiation. This method has been used in the literature on steels to measure hardness increase due to irradiation more accurately [6,7]. The results were compared to shear punch results tested after exposure to high energy proton and neutron irradiations performed at the SINQ facility at the Paul Scherrer Institute (PSI) in Switzerland and LANSCE proton beam line at Los Alamos National Laboratory (LANL) in the USA.

2. Experimental setup and analysis

2.1. Ion beam materials laboratory (IBML) irradiation and nanoindentation measurements

Two different Ta sheet materials (250 μm thick) were used in this experiment. Pure tantalum (Lot #A24M02) was purchased from Alfa Aesar. Ta with 1 wt% additional W (66% cold rolled) was received from Oak Ridge National Laboratory (ORNL). One sample of each material was used in the as-received condition and a second sample underwent a heat treatment. The heat treatment was 2 h at 1200 °C and 10^{-4} Torr vacuum. The sample was free standing in the furnace so it did not touch any of the furnace components. The end where the sample was held in place was cut off after the heat treatment. During this process ~400 ppm oxygen diffused into the Ta (see Table 1). After the heat treatment, the samples (as received and annealed) were sliced into six pieces and five were analyzed for their oxygen and nitrogen content using a LECO TC 600 ion spectrometer. The calibration for this instrument was done using titanium standard 501-653 and a zirconium standard 502-047. Also four additional reference samples which underwent the same heat treatment were analyzed using this process. The results of these measurements are presented in Table 1. Thus four different specimens were tested: pure Ta, as-received

* Corresponding author. Address: Los Alamos National Laboratory, P.O. Box 1663, Los Alamos, 87544 NM, USA. Tel.: +1 505 629 9893; fax: +1 505 667 7443.
E-mail address: peterh@lanl.gov (P. Hosemann).

0022-3115/$ - see front matter Published by Elsevier B.V.
doi:10.1016/j.jnucmat.2008.09.027

Table 1
Presents the oxygen content bulk hardness (micro and nanoindents), bulk *E*-modulus (gained by nanoindentation) and tensile test results.

Material	Oxygen content (ppm)	Standard deviation	Nanohardness bulk 200 nm indents (GPa)	Standard deviation	*E*-Modulus (GPa)	Standard deviation	Mic. Hard. Berkovic (MPa)	Mic. Hard. Vickers (MPa)	Yield strength (MPa)
Ta1W	106	50	3.39	0.17	174	4.1	2400	2099	600
Ta1W + O	360	35	3.85	1.60	182	3.6	1850	1570	
Ta	72	51	2.06	0.10	160	4.5	1050	921	210
Ta + O	377	38	3.60	1.14	176	3.2	2030	1660	

(Ta); Ta–1W, 66% cold worked (Ta1W); Ta annealed to pickup ~400 ppm O (Ta + O) and Ta1W annealed to pickup 400 ppm oxygen (Ta1W + O). After the annealing treatment, the remaining parts of the four samples were ground on both sides (last step 1200 grit) to ensure a flat and clean surface. The final thickness of the specimen was ~200 μm. The edges were ground and polished (last step 1 μm diamond polish) so the four samples fit side by side in the irradiation holder. The specimens were mounted on a copper sample holder using Ag paste to ensure good thermal and electrical conductivity. The copper sample holder was air cooled from the inside. The temperature on the Cu sample holder was monitored with a thermocouple on the Cu sample holder placed next to the samples (1–2 mm from the samples). The measured temperature stayed between 25 and 35 °C. Two strips of scintillators were mounted on top of the samples having a 2 mm gap in between to localize the beam on the samples (see Fig. 1b). The mounted samples were placed in the tandem accelerator located at LANL in the ion beam materials laboratory (IBML). The sample holder was electrically insulated from its surrounding beam line parts using Teflon plastic. Therefore it was possible to count the total amount of charged particles hitting the specimen. To induce the radiation damage a 3.5 MeV proton beam was used with a nominal current of about ~1 μA on target. The beam was rastered over a 2 mm × 4 mm surface area hitting all four samples at the same time. Therefore the total area irradiated on each sample was 1 mm × 2 mm. During the experiment (10 h irradiation time) a total of 2.25×10^{17} protons were counted. The amount of protons and the 8 mm^2 surface led to the depth dose profile shown in Fig. 2 using SRIM Monte Carlo simulation [8]. The damage in the near surface region (~10 μm) was ~0.5 dpa, in the deeper surface region (10–25 μm) was 0.5–1 dpa and in the particle stopping region (~35 μm) ~4.5 dpa. The total beam penetration depth was ~40 μm. After the irradiation experiment, the 200 μm wide sample edges were polished to finish with 1/10 μm diamond. The resulting RMS surface roughness measured using AFM on a 5 μm × 5 μm scan area was 5.6–10 nm. The polished samples were analyzed in a Hysitron nanoindenter machine (low load head with a maximum

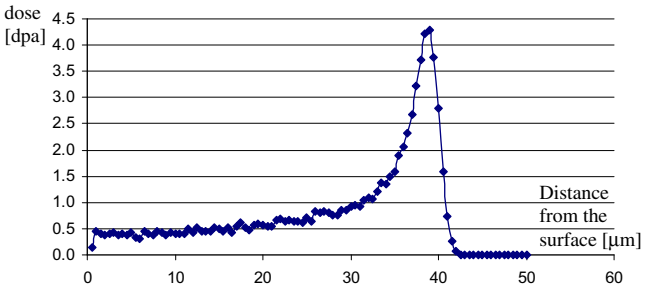

Fig. 2. Calculation results of dose vs. distance from the surface using SRIM.

load of 10 mN) using a Berkovich Indenter. On each sample, a raster of 12 rows and 10 columns of nanoindents were made (a total of 120 indents). Constant displacement mode to ~200 nm depth was used and the distance between the indents was ~4 μm (Fig. 3). To determine the hardness and *E*-modulus of the non-irradiated samples, seven indents in an H shaped array were made on each sample away from the irradiated area using the same indentation parameters. To determine the indentation size effect [12,13] the Hysitron high load head was used (maximum load 2 N) with a high load Berkovich tip and indentation depth vs. hardness curves were measured in the unirradiated area.

2.2. SINQ target irradiation program (STIP) II and LANSCE irradiations

About 3 mm diameter disks of pure Ta were put in the STIP II irradiation [9]. In this irradiation, the samples were placed in sealed stainless steel rods in the center of the SINQ spallation target. A 570 MeV proton beam interacts with this target to produce neutrons while uniformly irradiating the samples. The samples were irradiated in this target to a maximum dose of 21 dpa. The exact location of the samples and the known beam profile were used to determine the exact dose to which the samples were irradiated. The irradiation temperature was below 300 °C. Three millimeter

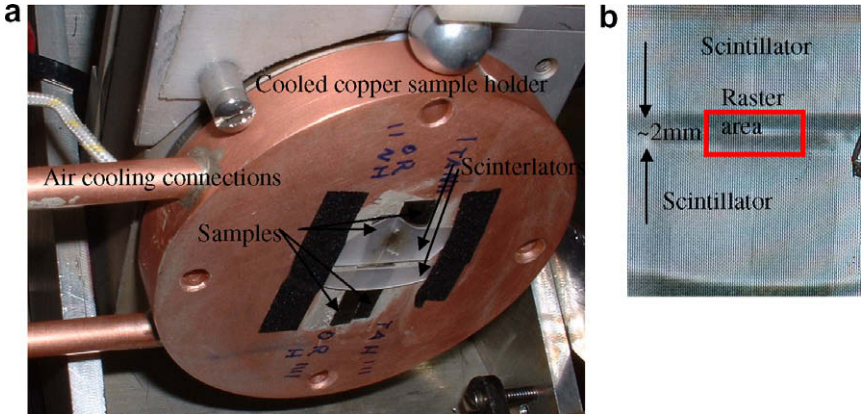

Fig. 1. The experimental setup in the beam line (a); view on the samples and the Scintillator through the beam line CCD camera (b).

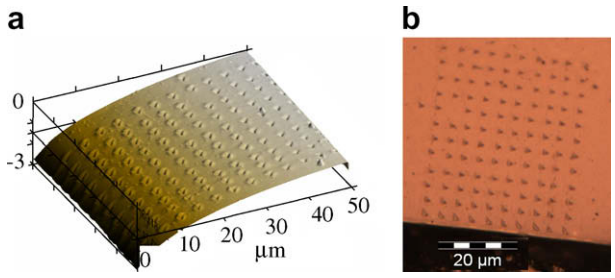

Fig. 3. (a) 50 × 50 μm 3D AFM image of the 10 × 12 indents array. The strong edge rounding is visible. *Z* range = 3 μm; (b) Optical image of the area shown verifies the distance from to the edge.

diameter disks of Ta1W (66% cold rolled) were irradiated in the LANSCE 800 MeV, 1 mA beam line. The samples were irradiated to doses up to 23 dpa in sealed, water cooled metal containers [10]. The irradiation time was ~6 months and the temperature ranged from 30 to 90 °C. After the samples were irradiated, shear punch tests were performed. The shear punch device is located in the Wing nine hot cells of the CMR building at LANL. Shear punch tests allow the determination of shear yield strength and a shear maximum strength. To correlate the data with tensile data, control tensile tests were performed on the as received Ta material at room temperature. The samples were wire EDM cut from the exact same sheet as the samples for the irradiation experiment. The specimen used was an S-1 tensile specimen with gage dimensions of 5 mm × 1.2 mm × 0.25 mm thick. The tensile tests were performed on an Instron machine at room temperature. Specimens were tested at an initial strain rate of 10^{-4}/s. Load and displacement were measured and converted to stress and strain. The stress/strain curve for each specimen was corrected for machine compliance. The compliance-corrected stress/strain curves were used to determine 0.2% offset yield stress, ultimate tensile strength and uniform elongation and used to relate to the properties measured from shear punch testing.

3. Results

3.1. Nanoindentation measurements on the IBML irradiated samples

The results of the oxygen analysis are given in Table 1. There it can be seen that the heat treated samples had a factor of 3–5 times higher oxygen content than the non-treated specimens. In Table 1 the hardness and Young's modulus of the bulk materials are presented as determined from the nanoindentation measurements. The values are averaged from seven indents measured at a location 100 μm away from the surface. The hardest material is the Ta1W + O specimen while the softest is the pure Ta sample. It is known [11–13] that nanoindentation measurements have higher values than a large scale hardness measurement would give because of the indentation size effect. For this reason, this data cannot be compared directly with micro- and macroscopic hardness values. Therefore calibration curves had to be done on the unirradiated sample by performing indentation depth vs. hardness measurements. The indentation depth was increased from ~100 to 3500 nm in steps. Seven indents of the same depth were performed. These calibration curves are shown in Fig. 4 along with the modeled hardness vs. indentation depth curves using the Nix and Gao model [12].

3.2. Shear punch measurements on LANSCE and STIP II irradiated samples

Shear punch measurements were performed on STIP II irradiated Ta specimens and LANSCE irradiated Ta1W specimens at room temperature. The total dose of these specimens was up to 23 dpa. Each test produced a shear stress vs. shear displacement curve. Shear yield stress was measured from each curve and yield strength was calculated from the shear yield strength measurements with a factor of 1.77 [14]. Fig. 5 presents the shear punch results of these alloys tested in a uniform neutron flux. It can be seen that the Ta1W yield strength increase is less with irradiation than the pure Ta irradiated in STIP II.

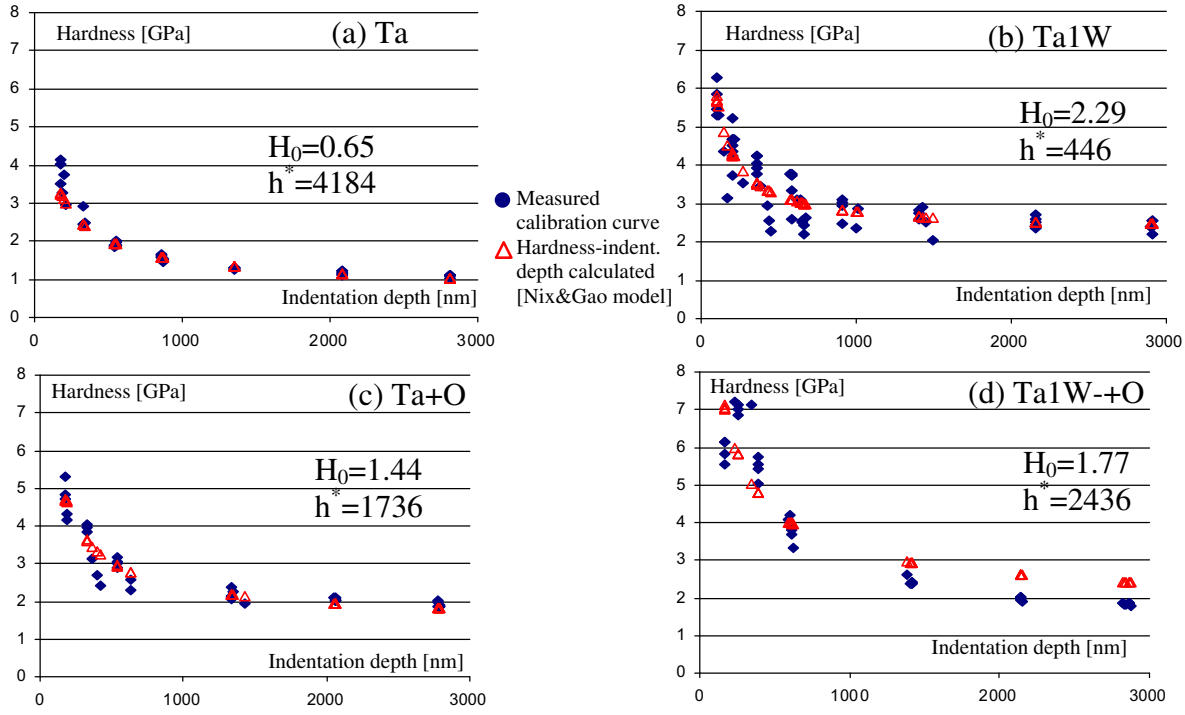

Fig. 4. Calibration curves (a) Ta–AR, (b) Ta1W–AR, (c) Ta–ANL and (d) Ta1W–ANL.

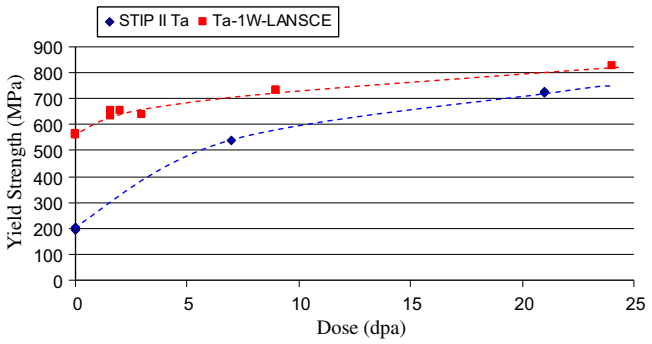

Fig. 5. The yield strength calculated from shear yield strength data from the STIP II (Ta) and LANSCE (TA1W) experiments.

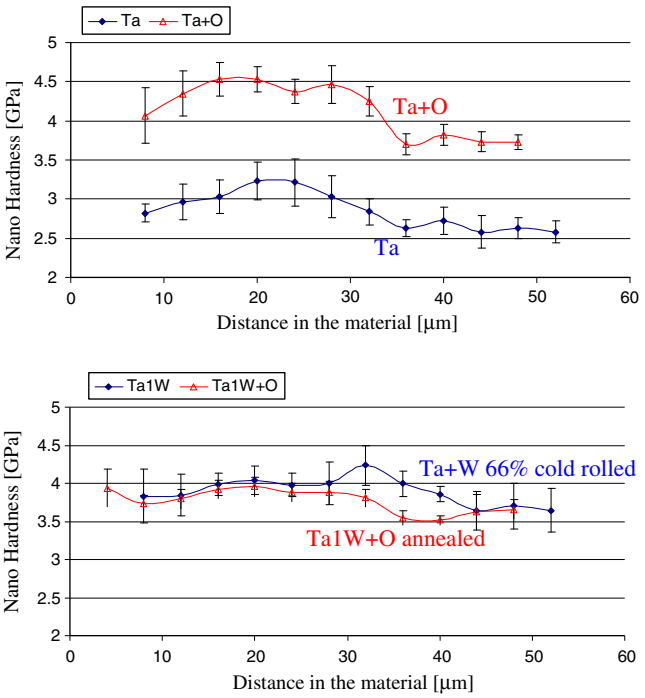

Fig. 6. The standardized hardness results are shown for the four tested Ta materials.

4. Discussion

The oxygen measurements correlate with the Ta–O phase diagram [5] where a high solubility of oxygen in tantalum is shown at elevated temperature. In [15–17] the O enrichment in Ta vs. gas pressure, temperature and Ta-alloy is reported. Although the Ta there was not treated under the exact same conditions used in this experiment (different temperatures, different gas pressures), it can be seen that the oxygen content reported is in a similar range as observed here. By removing 20–50 μm from the samples surface and cutting of the ends of the Ta sheet it was assured that the sample material was not contaminated with other impurities than O, after the heat treatment. The Leco elemental analysis also showed that the N content is not significantly higher in the annealed material than in the as received material.

The nanohardness results showed initially that the Young's modulus increases in the region near the surface, and the hardness increases to a lesser extent near the surface region. It is known that the Young's modulus of a material does not change during low energy proton irradiation. Therefore, it can be stated that the higher E-modulus readings towards the surface result from surface stress and edge effects. Since the Young's modulus values appear to be inaccurate, the measured hardness values also need to be corrected. Assuming that the Young's modulus (E-modulus) is constant throughout the entire material, a new corrected indentation area is calculated using:

$$A_{\text{corrected}} = A_{\text{measured}}(E_{\text{measured}}/E_{\text{bulk}})^2 \quad (1)$$

The assumed E_{bulk} is the Young's modulus measured deep in the material (100 μm away from the surface and radiation area).

This new $A_{\text{corrected}}$ is used to calculate the corrected hardness by using:

$$H_{\text{corrected}} = \text{Force}_{\text{applied}}/A_{\text{corrected}} \quad (2)$$

This method has been previously shown to give accurate corrected contact areas in metals with known residual stress [18]. The nanoindents were 200 nm deep and ~1 μm in lateral direction. These relatively large indents should not be affected by any surface stress or damage caused by the preparation. The corrected hardness values across the sample cross-section are presented in Fig. 6. The shape of each curve follows the dose vs. distance calculation in Fig. 2. The first two rows of indents (up to 8 μm–10 μm distance from the edge) were not used for any calculation or a diagram since the indents there are not triangular shaped and the rounding of the edge effects the measurements. A trend of hardness increase in all four materials to about 30 μm in depth can be seen. The hardness drops then further into the material. Quantitative analysis of the nanohardness data shows noticeable hardening in the pure Ta and Ta + 1W alloys due to irradiation. These results show that the Ta1W (66% cold rolled) is twice as hard as the Ta in the unirradiated area. Ta1W + O and Ta1W (cold rolled) have similar hardnesses within the uncertainty. Therefore, it appears that the high defect density caused by the cold rolling anneals out (due to the 1200 °C heat treatment) while the additional oxygen causes an additional hardness increase. The irradiation dose seems to have less of an effect on the Ta1W-(cold rolled) alloy than on the pure Ta which can be explained by the higher defect density due to the cold rolling and the O and W additions which can act as defect sinks. But to explain this behavior in detail, TEM analyses need to be performed. The measurements which demonstrate the indentation size effect [13] (Fig. 4) show that the cold rolled material has much more data scatter which might be based on the fact that the local dislocation density varies strongly because of the rolling deformation. The fit for the size effect curves shown in Fig. 4 was performed using the Nix and Gao model [12]. As it is shown, the model does not fit very well with the data. Also the calculated H_0 and h^* are not in very good agreement with the measured data. For irradiated salt crystals, hardness results [19] show a similar disagreement with the Nix and Gao model. The reason for the disparity was attributed to a different hardening mechanism [19]. Irradiation primarily induces point defects, which block dislocation motion and increase hardness, but not with the same square root dependence that results from dislocation–dislocation interactions, which is the hardening mechanism modeled in the Nix and Gao model [10]. But since there are no better models available, the Nix and Gao model was used to correlate the nanoindentation data to micro indentation data using:

$$H/H_0 = (1 + h^*/h)^{0.5} \quad (3)$$

where H_0 is the hardness in the limit of infinite depth and h^* is a characteristic depth dependent on the shape of the indenter [10].

Using the nanohardness measurements performed here and the calibration curves from Fig. 4, the Berkovich microhardness increase due to O in the unirradiated area is found to be ~1000 MPa for pure Ta and not significant for the for the Ta1W (cold rolled).

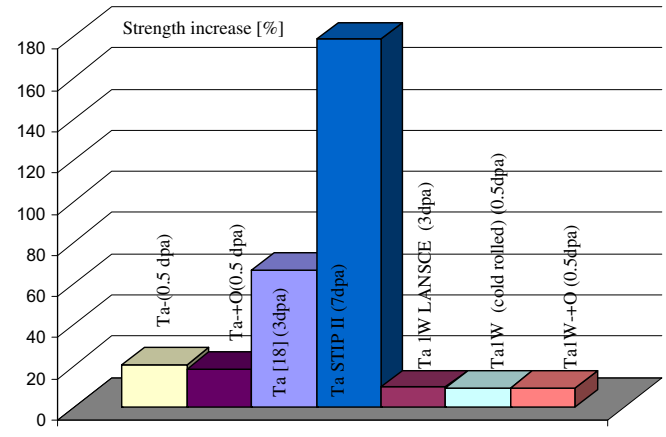

Fig. 7. This bar graph plots the increase in strength (measured through hardness and shear punch testing) quantified in percent at different doses for various irradiation experiments.

The radiation induced hardness increase is the highest in the Ta + O material while Ta1W + O and Ta1W (cold rolled) show the lowest which could be caused by the defect sinks, present in the high defect density on the cold rolled and the O added materials. Fig. 7 presents a comparison of the hardness increase due to irradiation of the four IBML tested Ta materials and the STIP and LANSCE irradiated alloys. This bar graph shows a relative strength increase (in percent) to the unirradiated condition. It can be seen that the Ta1W-(cold rolled) and Ta1W + O samples show similar strength increases at 0.5 dpa and very little additional increases in strength are observed for additional dose to 3 dpa. Also the Pure Ta and Ta + O IBML irradiated materials show similar strength increases at 0.5 dpa but additional dose to 3 dpa using Cu ions [20] and 7 dpa from STIP irradiation results in additional increases in strength. Thus, it appears that the defect density has saturated in the Ta1W material after only 0.5 dpa but this is not evident in the pure tantalum where the strength continues to increase up to 7 dpa exposure.

5. Conclusions

- The irradiation induced hardening in pure Ta, oxygen doped Ta, 66% cold rolled Ta1W and oxygen doped Ta1W was tested and quantified using low energy protons followed by nanoindentation on the sample cross-section. It is shown that similar to what is reported in the literature cross-section nanooindentation can be used to measure the hardness increase due to irradiation.
- It was found that only 400 wppm of oxygen in Ta can cause a significant hardness increase and therefore ductility decrease. The hardening observed from oxygen in tantalum is in agreement with the literature. This lead to the conclusion that if Ta is used as structural component it has to be ensured that the environment is at low temperature (to avoid oxygen pickup) and/or oxygen free.
- It was found that the addition of W leads to a smaller percentage (compared to initial yield stress) hardness increase due to irradiation as well as a much smaller percentage hardness increase due to oxygen content increase. The effects of the addition of W on ductility changes were not investigate which may show different trends.
- The nanoindentation data and shear punch data follow the same trend of property changes. The Ta1W material seems to harden less than the pure Ta material with dose.

Acknowledgements

Mark Hollander and Yongqiang Wang are gratefully acknowledged for supporting the accelerator irradiation. Ken Farrell of ORNL for providing the Ta1W material.

References

[1] J. Chen, H. Ullmaier, T. Flossdorf, W. Kühnlein, R. Duwe, F. Carsughi, T. Broome, J. Nucl. Mater. 298 (2001) 248.
[2] J. Chen, G.S. Bauer, T. Broome, F. Carsughi, Y. Dai, S.A. Maloy, M. Roedig, W.F. Sommer, H. Ullmaier, J. Nucl. Mater. 318 (2003) 56.
[3] R.D. Brown, M.S. Wechsler, C. Tschalaer, Effect of radiation on material properties, in: F.A. Garner, C.H. Henager, N. Igata (Eds.), 13th International Symposium (Part II), ASTM STP 956, Philadelphia, PA, American Society for Testing of Materials, 1987, p. 131.
[4] R.D. Brown, J.R. Cost, in: 11th International Symposium on Effects on Materials, American Society for Testing and Materials, Scottsdale, Arizona, 1982.
[5] S.P. Garg, N. Krishnamurthy, A. Awasthi, M. Venkatraman, J. Phase Equilib. 17 (1996) 63.
[6] P. Hosemann, J.G. Swadener, D. Kiener, G.S. Was, S.A. Maloy, N. Li, J. Nucl. Mater. 375 (2008) 135.
[7] P. Hosemann, C. Vieh, R.R. Greco, S. Kabra, J.A. Valdez, M.J. Cappiello, S.A. Maloy, J. Nucl. Mater. (in press).
[8] SRIM software. <http://www.srim.org/>.
[9] Y. Dai, X. Jia, R. Thermer, D. Hamaguchi, K. Geissmann, E. Lehmann, H.P. Linder, M. James, F. Gröschel, W. Wagner, G.S. Bauer, J. Nucl. Mater. 343 (2005) 33.
[10] S.A. Maloy, W.F. Sommer, M.R. James, T.J. Romero, M.R. Lopez, E. Zimmermann, J.M. Ledbetter, Nucl. Technol. 132 (2000) 103.
[11] J.G. Swadener, E.P. George, G.M. Pharr, J. Mech. Phys. Solids 50 (2002) 681.
[12] W.D. Nix, H. Gao, J. Mech. Solids 46 (1998) 411.
[13] F. Schulz, H. Hanemann, Z.F. Metallkunde 33 (1941) 124.
[14] R.K. Guduru, K.A. Darling, R. Kishore, R.O. Scattergood, C.C. Koch, K.L. Murty, Mater. Sci. Eng. 395 (2005) 307.
[15] S. Stecura, Oxidation of Metals vol.10 (5) (1976).
[16] E. Gebhardt, H.D. Seghezzi, Z.f. Metallkunde 50 (1959) 521.
[17] E. Gebhardt, H.D. Seghezzi, Z.f. Metallkunde 48 (1957) 503.
[18] T.Y. Tsui, W.C. Oliver, G.M. Pharr, J. Mater. Res. 11 (1996) 752.
[19] J.G. Swadener, A. Misra, R.G. Hoagland, M. Nastasi, Scripta Mater. 47 (2002) 343.
[20] K. Yasunaga, H. Watanabe, N. Yoshida, T. Muroga, N. Noda, J. Nucl. Mater. 283–287 (2000) 179.